Actinomycin D Binds to d(TGTCATG) with 2:1 Drug to Duplex Stoichiometry†

Fu-Ming Chen* and Feng Sha

Department of Chemistry, Tennessee State University, Nashville, Tennessee 37209-1561

Received September 11, 2001

ABSTRACT: Despite the apparent single-stranded conformation and the absence of a GpC site, d(TGTCATTG) has been found to bind strongly to actinomycin D (ACTD) with 1:1 drug to strand binding stoichiometry. A hairpin binding model was speculated in which the planar phenoxazone chromophore inserts at the GTC site by pushing out the T-base while the terminal G folds back to form a G·C base pair so that the 3′-sides of both G-bases stack on the opposite faces of the phenoxazone plane. However, it was also suggested that a slipped duplex binding with similar binding principle could also be operative at higher DNA concentrations. To support such a contention, ACTD binding studies were made with d(TGT**CATG**) and related oligomers. This heptamer differs from the parent octamer d(TGTCATTG) by a mere removal of a T-base which should result in an enhancement of dimeric duplex formation and a concomitant reduction in monomeric hairpin contribution. It was found that ACTD binds well to d(TGT**CATG**) with 1 drug to 1 strand (or 2 drugs to 1 duplex) binding stoichiometry. These results are consistent with a slipped duplex binding model in which a dimeric duplex is formed at the self-complementary CATG tetranucleotide sequence with extruding TGT ends. Two drug molecules are bound at both ends of the duplex by pushing out the T-bases of GTC's so that the opposite faces of each phenoxazone are stacked by the 3′-sides of the two G-bases on opposite strands. Such a model provides a ready explanation for the observed enhancement in ACTD binding to d(TGT**CATG**TC) and d(TGT**CATG**TCA), where additional base pairs at the ends will stabilize GTC/GTC binding sites, and to d(TGT**CAATTG**) in which two additional base pairs facilitate the slipped-duplex formation. The observed ACTD affinity reductions for oligomers containing GTTC instead of GTC are also consistent with the T-base displacement model. These findings greatly expand the repertoire of ACTD binding to DNA and may have important implications on understanding the transcription inhibitory activities of this drug.

Actinomycin D (ACTD)[1] is one of the most extensively studied drugs, and its widespread interest stems from its function as an antitumor agent and as a model sequence-specific antibiotic. It consists of a planar 2-aminophenoxazin-3-one chromophore and two bulky cyclic pentapeptide lactones (see Figure 1). The drug exerts its biological function via inhibition of transcription in a wide variety of systems. It binds to duplex DNA via intercalation with high affinity and dissociates slowly from DNA, which had led to a suggested mechanism whereby the drug blocks the progression of RNA polymerase along the template DNA to terminate the transcription (*1*). The DNA binding of ACTD is quite sequence-specific and has been shown to prefer greatly the duplex GpC site. This base-sequence-specificity derives mainly from the formation of strong hydrogen bonds in the minor groove, between the N-2 amino group and N-3 ring nitrogen of the two guanine residues with the carbonyl oxygen atoms and amide groups of threonine residues of the cyclic peptapeptides, respectively (*2, 3*). These essential drug−DNA hydrogen bonds are protected by the cyclic pentapeptides, which effectively shield them from solvent exposure. The size of the four-base-paired binding site suggests that the binding characteristics of ACTD to the GpC site may be affected by the adjacent flanking base pairs. Indeed, our studies with self-complementary (*4*) as well as non-self-complementary (*5*) -XGCY-containing oligomers revealed that the binding affinity and dissociation kinetics of this drug from DNA are, indeed, greatly affected by the nature of the adjacent X and Y bases. For example, ACTD binds strongly to and dissociates very slowly from the -TGCA- site, whereas it binds weakly and dissociates very rapidly from the -GGCC- sequence (*4*). These studies were subsequently extended to include the effects of flanking base mismatches on the affinity and kinetic behavior of the GpC sequence. It was found that ACTD binds well to and

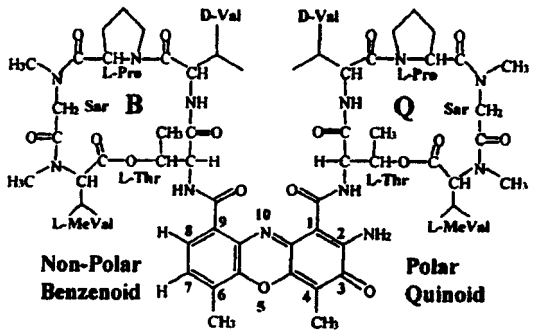

FIGURE 1: Chemical structure of actinomycin D.

† This research was supported by a subproject of Minority Biomedical Research Support (MBRS) Grant S06GM0892.

* To whom correspondence should be addressed. Tel: (615)963-5325, FAX: (615)963-5434, E-Mail: fchen@tnstate.edu.

[1] Abbreviations: ACTD, actinomycin D; 7-AM-ACTD, 7-amino-actinomycin D; CD, circular dichroism.

10.1021/bi011787o CCC: $22.00
Published on Web 03/20/2002

dissociates slowly from the GpC site with adjacent pyrimidine/pyrimidine mismatches, especially those of T/T mismatches (*6*).

Although the GpC sequence-specificity and the effects of adjacent bases on ACTD binding appear to be well characterized, there have been reports to indicate that this drug may also bind strongly to some non-GpC-containing sequences (*7*−*9*) and even to some single-stranded DNA (*10*−*14*). In particular, it has been reported that ACTD binds strongly and cooperatively to a self-complementary but non-GpC-containing octamer, d(CGTCGACG), with a 2:1 drug-to-duplex ratio (*7*). In subsequent studies, our laboratory found that d(CGTCGTCG) and d(CGACGACG) also bind strongly to ACTD despite their lack of self-complementarity (*15*). Further base-replacement studies with d(CGTCGTCG) led us to uncover that ACTD binds strongly to the sequence d(TGTCATTG) which is of apparent single-stranded conformation (*16*). Such a finding is significant and may have relevance in ACTD binding to single-stranded DNA in general. A hairpin-like binding mode was speculated for such a binding, wherein the phenoxazone chromophore of ACTD inserts at the GTC site with the T-base being pushed out whereas the 3′-terimus G folds back to form a base pair with the internal C and stacks on the opposite face of the chromophore. A possible minor contribution from ACTD binding to a slipped dimeric duplex was also suggested, utilizing the same binding principle of the 3′-sides of two G-bases stacking on opposite faces of the phenoxazone plane. The main purpose of this report is to demonstrate that ACTD can, indeed, bind strongly via the slipped-duplex binding mode to some DNA sequences that are devoid of GpC sites. Understanding the ACTD binding to sequences which do not contain the classic GpC sites will provide considerable insights into its modes of DNA binding and may assist in uncovering other new strong ACTD binding sequences. The findings from such studies may also have important implications in understanding the mechanism of inhibitory action of this drug on the transcription processes.

MATERIALS AND METHODS

Synthetic oligonucleotides were purchased from ResGen (Huntsville, AL) and used without further purification. These oligomers were purified by the vendor via reverse-phase oligonucleotide purification cartridges and exhibited single-band electrophoretic mobilities in denaturing polyacrylamide gel electrophoresis with stated purity of ≥95%. Concentrations of the DNA solutions (in nucleotide) were determined by measuring the absorbances at 260 nm after melting (at 95 °C). The extinction coefficients of DNA oligomers were obtained via nearest-neighbor approximation using mono- and dinucleotide values tabulated in Fasman (*17*). ACTD and 7-amino-ACTD (7-AM-ACTD) were purchased from Serva. Concentrations of the drug solutions were determined by measuring the absorbances at 440 nm (for ACTD) and 528 nm (for 7-AM-ACTD), using extinction coefficients of 24 500 and 23 600 cm^{-1} M^{-1}, respectively. Stock solutions for oligonucleotides and drugs were prepared by dissolving in 10 mM Tris−borate buffer solution of pH 8 containing 0.1 M NaCl and 1 mM $MgCl_2$. Absorption spectra were measured with a Cary 1E spectrophotometric system. Absorption spectral titrations were carried out by starting with a 5 μM ACTD solution of 2 mL followed by progressive additions of the oligomer stock at equal time intervals. Absorbance differences between 427 and 480 nm during absorption spectral titrations were used to obtain the binding isotherms.

Association binding constants (K) were extracted via nonlinear least-squares fits on the experimental binding isotherms using the 1:1 drug to strand binding model: D + S = DS, where D, S, and DS are free drug, free single-stranded DNA, and drug−DNA complex, respectively. By means of equations for the mass balances of drug and DNA (in strand), the following equations can be derived:

$$D^2K + D[KD_t(X - 1) + 1] = D_t$$

$$S = D_t(X - 1) + D$$

$$Y = (\epsilon_D + \epsilon_1 KS)D/D_t$$

where $X \equiv S_t/D_t$, and ϵ_D and ϵ_1 are the extinction coefficients of the free and bound drugs, and D_t and S_t are the total drug and DNA strand concentrations, respectively, at each point of the titration. Experimental binding isotherms were plotted as the apparent extinction coefficient (Y) vs X, and nonlinear least-squares fits with the above equations were made by initially fixing the known ϵ_D and subsequently relaxed to obtain the best fit to extract the binding constant K. The nonlinear least-squares fit program of Micromath (Salt Lake City, UT) was used for our fitting purpose.

Attempts were also made to fit the binding isotherms to a more complicated model including the equilibrium between single strands and duplex, and the duplex binding to first and second drug molecules with respective binding constants of K_1 and K_2. Such a complex model requires finding roots for a sixth-order polynomial, and the nonlinear least-squares fits produced discontinuities with X around 1, likely the consequence of not discarding the roots with complex numbers in the program. A Simplex optimization using MATLAB was then attempted with constraints to discard those complex roots which resulted in good fit for all the data range. However, such an approach was not fruitful since the fit requires the evaluation of six parameters and the program is frequently trapped in local minima. Despite the fact that excellent fits with very reasonable extinction coefficients for the free and bound drugs can be obtained, the three extracted equilibrium constants vary significantly even with a slight change in the initial guesses. Since excellent fits were obtained with the simpler 1:1 drug to strand binding model for nearly all the isotherms, no further attempts were made with the more complicated model. The binding constant K obtained via the 1:1 model can be regarded as the geometric mean of K_1 and K_2, i.e., $K \approx (K_1K_2)^{1/2}$.

RESULTS

Actinomycin D Binds to d(TGTCATG) with 2:1 Drug to Duplex Binding Stoichiometry. The heptamer d(TG*T***CATG**) differs from the octamer d(TGTCATTG) studied earlier by the mere removal of a T-base from the CATTG portion to form an oligomer that contains a CATG self-complementary sequence. This should result in an enhancement of the dimeric duplex formation and a concomitant reduction of the monomeric hairpin contribution. The ACTD binding

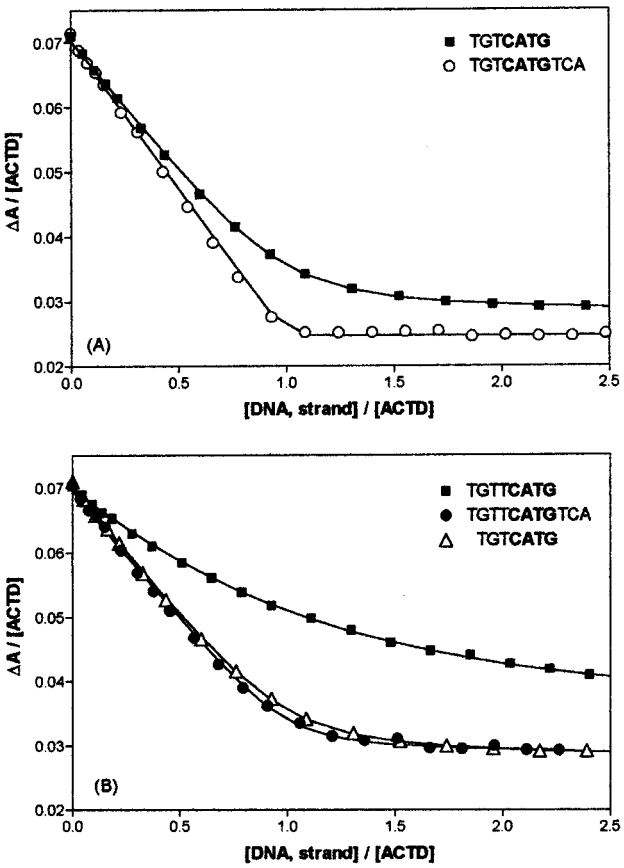

FIGURE 2: Comparison of equilibrium binding isotherms at 25 °C for ACTD binding to oligomer derived from appending the 3′-terminus with TCA to d(TG*T***CATG**) (panel A) and to d(TG*T*-*T***CATG**) (panel B). Δ*A* is the absorbance difference between 427 and 480 nm. Both ACTD and DNA strand concentrations are in μM. Solid lines are the nonlinear least-squares fitted curves using the 1:1 drug to strand binding model as described in the text, and the extracted binding constants are shown in the tables.

Table 1: Comparison of Binding and Melting Parameters of d(TGTCATG) and Its 3′-Terminus Appended Derivatives[a]

oligomer	K (μM^{-1})	T_m^0 (°C)	T_m (°C)
d(TG*T***CATG**)	4.9 ± 0.3		51
d(TG*T***CATG**T)	3.4 ± 0.7		50
d(TG*T***CATG**TC)	~100		61
d(TG*T***CATG**TCA)	~100		67
d(TG*T***CATG**A)	2.5 ± 0.3		46
d(TG*T***CATG**AC)	4.1 ± 0.8	32	60
d(TG*T***CATG**ACA)	6.5 ± 2.2	34	62

[a] Equilibrium titrations were carried out at 25 °C, and the binding constant K is obtained via nonlinear least-squares fit to the experimental isotherm using the simple 1:1 drug to strand binding model. T_m^0 and T_m are melting temperatures of 40 μM DNA (in nucleotide) containing 0.1 M NaCl in the absence and in the presence of 7 μM ACTD, respectively. The melting profiles were obtained via 275 nm absorbance monitoring.

isotherms of d(TG*T***CATG**) along with that of d(TG*T***CAT-G**TCA) are shown in Figure 2A. The saturation patterns of these isotherms suggest a 1:1 drug to strand (or 2:1 drug to duplex) binding stoichiometry. Thus, the experimental binding isotherms were fitted with a nonlinear least-squares method using the 1:1 binding model, and the extracted binding constants for related oligomers are summarized in Table 1. The ACTD binding affinity for d(TG*T***CATG**) is found to be 4.9×10^6 M^{-1}, and the fit (solid curve in the figure) can be seen to be excellent, reaffirming the plausibility of such a binding model. To account for the 2:1 drug to duplex binding complex, a binding model is speculated in which a dimeric duplex stem is formed at the CATG sequence with extruding TGT on both sides of the duplex stem. The ACTD molecules then bind at both ends of the slipped duplex, where one face of each phenoxazone chromophore is stacked by the G·C base pair while the other face is stacked by the 3′-side of the G-base of G*T*C with a looped-out *T*-base (see schematic drawing in Figure 3a).

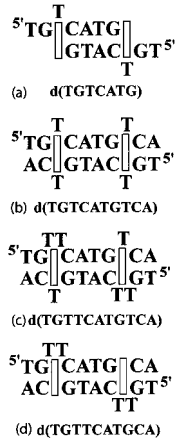

FIGURE 3: Schematic drawings of the proposed slipped-duplex binding model of ACTD binding to some representative oligomers. The rectangular block represents the phenoxazone ring (chromophore) of ACTD.

ACTD Affinities Are Dramatically Enhanced by TC and TCA Additions at the 3′-Terminus. The efficacy of such a binding mode may be affected by adding bases to the 3′-end, especially those that facilitate the dimeric duplex formation. ACTD binding studies were thus made with T, TC, and TCA appended to the 3′-terminus of d(TG*T***CATG**). A model fitted binding constant (see Table 1) of 3.4×10^6 M^{-1} was found for d(TG*T***CATG**T), whereas about 100×10^6 M^{-1} was found for both d(TG*T***CATG**TC) and d(TG*T*-**CATG**TCA). Thus, the addition of a T-base at the 3′-end has only a minor effect (slight reduction) on its ACTD binding, whereas the additions of TC and TCA significantly enhanced their binding affinities. Such dramatic order of magnitude enhancements in ACTD affinities may be attributed to the extra base pair(s) formed at the ends to facilitate the formation of G*T*C/G*T*C sites, where the ACTD binding supposedly occurs via *T*-base displacements. The binding isotherms for d(TG*T***CATG**TC) and d(TG*T***CATG**-TCA) are nearly identical, and only that of the latter is included in Figure 2A for comparison. The 1:1 drug to strand (or 2:1 drug to duplex) binding stoichiometry for this oligomer is clearly evident from the saturation pattern of its binding profile. The schematic drawing of its speculated ACTD binding is shown in Figure 3b.

The role of base displacements on ACTD binding to the G*T*C/G*T*C site was further investigated by studying ACTD binding behaviors of oligomers derived from appending A, AC, and ACA to the 3′-end of d(TG*T***CATG**). These base additions should result in the formation of duplex stems with progressive increase in the number of base pairs. It is apparent from a comparison of binding isotherms of these oligomers (not shown) that the ACTD binding enhancements due to AC and ACA additions are much less dramatic than

Table 2: Comparison of Binding and Melting Parameters of Some Oligomers Containing the GTTC Sequence[a]

oligomer	K (μM^{-1})	T_m^0 (°C)	T_m (°C)
d(TG***T*CATG**)	4.9 ± 0.3		51
d(TG***TT*CATG**)	0.35 ± 0.02		42
d(TG***TT*CATGT**)	0.24 ± 0.03		32
d(TG***TT*CATGTC**)	2.9 ± 0.5		48
d(TG***TT*CATGTCA**)	11.2 ± 2.5		55
d(TG***TT*CATGCA**)	8.3 ± 1.6		54
d(TG***T*CATGCA**)	25.5 ± 3.7		63
d(TG**CATG*T*CA**)	88 ± 70	30	59

[a] Equilibrium titrations were carried out at 25 °C, and the binding constant K is obtained via nonlinear least-squares fit to the experimental isotherm using the simple 1:1 binding model. T_m^0 and T_m are melting temperatures of 40 μM (in nucleotide) DNA/0.1 M NaCl in the absence and in the presence of 7 μM ACTD, respectively. The melting profiles were obtained via 275 nm absorbance monitoring.

those of TC and TCA additions. Binding constants (see also Table 1) of 2.5×10^6, 4.1×10^6, and 6.5×10^6 M^{-1} were found for d(TG***T*CATG**A), d(TG***T*CATGA**C), and d(TG***T*CATG**ACA), respectively. These values are lower than those of the T, TC, and TCA appended counterparts, especially the last two, and may be attributed to differences in the nature of G*T*C/G*T*C vs G*T*C/G*A*C sites, a consequence of the *T*·*A* base pair formation of the latter. The progressive base additions resulted in dimeric duplex formation with 6-, 7-, and 8-base-paired duplex stems (underlined bases), respectively. Base displacements of the *T*·*A* base pair at the G*T*C/G*A*C duplex sites should be somewhat more difficult than those of the *T*/*T* mismatches at the G*T*C/G*T*C sites. This may account for the fact that even though the ACTD affinities of d(TG*T*CATG**AC**) and d(TG*T*CATG**ACA**) are still quite considerable, they are nearly an order of magnitude lower than those of d(TG*T*CATG**TC**) and d(TG*T*CATG**TCA**).

*ACTD Binding Affinity for d(TG**TT**CATG) Is Considerably Weakened.* If the binding at the G*T*C/G or G*T*C/G*T*C site requires *T*-base displacements, it is reasonable to suspect significantly weaker binding at the G*TT*C/G and G*TT*C/G*T*C sites because of the need to form a 2-T bulge to bring in the G-base during their ACTD binding. Thus, binding studies were also made with the corresponding oligomers where the G*T*C is replaced by G*TT*C. The extracted quantitative binding constants for these oligomers are included in Table 2 for comparison. The binding constant for d(TG***TT*CATG**T) was found to be 0.24×10^6 M^{-1}, which is slightly lower than that of 0.35×10^6 M^{-1} for d(TG***TT*CATG**), whereas the values of 2.9×10^6 and 11×10^6 M^{-1} were found for d(TG***TT*CATG**TC) and d(TG***TT*CATG**TCA), respectively, which are more than an order of magnitude higher than those of the two shorter oligomers but are roughly an order of magnitude lower than their G*T*C counterparts (compare with Table 1). The much weaker ACTD affinities seen for the G*TT*C series as compared to the G*T*C counterparts are consistent with the fact that a 2-base displacement is significantly more difficult than that of a single base. The binding isotherm of d(TG***TT*CATG**TCA) is compared with d(TG***TT*CATG**) along with d(TG***T*CATG**) in Figure 2B. It is interesting to note that the addition of TCA at the 3′-end has nearly compensated the binding diminution resulting from an additional T-base insertion at the GTC site. The schematic drawing for the speculated ACTD binding to d(TG***TT*CATG**TCA) is shown in Figure 3c.

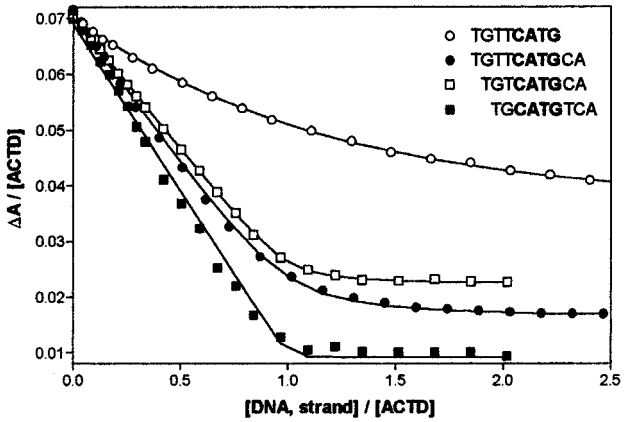

FIGURE 4: Comparison of equilibrium binding isotherms of ACTD at 25 °C for d(TG***TT*CATG**), d(TG***TT*CATG**CA), d(TG***T*CATGCA), and d(TG**CATG*T*CA). Solid lines are the nonlinear least-squares fitted curves using the 1:1 drug to strand binding model as described in the text, and the extracted binding constants are shown in the tables.

Interesting Tests on the Proposed Binding Mode. Interestingly, the addition of CA at the 3′-end of d(TG***TT*CATG**) to form the oligomer d(TG***TT*CATG**CA) led to an enhancement of nearly 20-fold in the ACTD affinity, exhibiting a binding constant of 8.3×10^6 M^{-1} but still retaining the 2:1 drug to duplex binding stoichiometry (see Table 2). This is consistent with our suggested binding model and can be attributed to the duplex formation of d(TG***TT*CATG**CA) at the *TT*-less self-complementary sequence to result in easier *TT* bulge formation for ACTD binding at the G*TT*C/GC sites. If such is indeed the case, considerable ACTD binding enhancement should be expected for d(TG***T*CATG**CA) since single-base displacement from the duplex would be easier than that of a 2-T bulge formation. Indeed, ACTD binding affinity for d(TG***T*CATG**CA) is found to be 26×10^6 M^{-1}, severalfold higher than the corresponding *TT*-oligomer. A related sequence, d(TG**CATG**TCA), is also found to bind strongly to ACTD with a roughly similar binding constant. Their binding isotherms are compared in Figure 4 , and the distinct leveling off at the 1:1 drug to strand (or 2:1 drug to duplex) ratio is particularly noteworthy.

The above results, especially the 2:1 drug to duplex binding stoichiometry, are in conformity to our proposed binding principle. The test for such a binding mode is, in fact, quite stringent for these three oligomers. The sequence d(TG**CATG***T*CA), similar to d(TG***T*CATG**CA) and d(TG***TT*CATG**CA), can form dimeric duplex at either the TGCA or the **CATG** sequence. It is generally expected that in the presence of ACTD the TGCA duplex will predominate because of the strong binding propensity of this site. If such were to be the case, a 1:1 drug to *duplex* binding stoichiometry would have been expected. However, if our proposed binding principle is valid, the CATG duplex will be favored in solutions of higher drug concentrations because such a duplex will enable the binding of two drug molecules to a duplex. The additional stabilization due to the binding of a second drug molecule should shift the equilibrium to favoring this duplex form. Indeed, our binding titrations indicate that both d(TG**CATG***T*CA) and d(TG***T*CATG**CA) exhibit binding constants of greater than 25×10^6 M^{-1} and a binding density of 2 drugs to 1 duplex, strong support for the notion that ACTD molecules are bound at the two GC/G*T*C sites

Table 3: Comparison of Binding and Melting Parameters for Oligomers of the Sequence Motif d(TGTCxyy′x′G)[a]

oligomer	K (μM^{-1})	T_m^0 (°C)	T_m (°C)
d(TG***T*CAATTG**)	12 ± 2		49
d(TG***T*CATATG**)	16.9 ± 5.0		54
d(TG***T*CACGTG**)	16.2 ± 2.4		54
d(TG***T*CTATAG**)	11.2 ± 2.1		52
d(TG***T*CTTAAG**)	23 ± 16		52
d(TG***T*CTCGAG**)	8.0 ± 1.6	26	52

[a] Equilibrium titrations were carried out at 25 °C, and the binding constant K is obtained via nonlinear least-squares fit to the experimental isotherm using the simple 1:1 binding model. T_m^0 and T_m are melting temperatures of 40 μM (in nucleotide) DNA/0.1 M NaCl in the absence and in the presence of 7 μM ACTD, respectively. The melting profiles were obtained via 275 nm absorbance monitoring.

with swing-out *T*-bases instead of binding at the canonical TGCA site. The schematic drawing of speculated ACTD binding to d(TGTT**CATG**CA) is shown in Figure 3d.

*Studies with d(TGT**CTAG**) Analogues*. Studies were also carried out with d(TG*T***CTAG**) and related oligomers (results not shown). Analogous to the CATG sequence, CTAG is also self-complementary. A dimeric duplex formation is, thus, expected at this sequence, and similar ACTD binding principle should also be applicable. Indeed, binding trends similar to those observed for the CATG series are also apparent in the CTAG series. For example, the ACTD affinities for TC and TCA additions at the 3′-terminus have been enhanced by more than an order of magnitude, whereas those of d(TG*T***CTAG**T) and d(TG*T***CTAG**A) are not greatly different from each other or from that of d(TGT**CTAG**). However, those of d(TG*T***CTAG**AC) and d(TG*T*CTA-GACA) are considerably weaker than the corresponding d(TG*T***CTAG**TC) and d(TG*T***CTAG**TCA), respectively, supporting the notion that *T*·*A* base pair formation at the G*T*C/G*A*C site somewhat hinders their base displacements from the duplex in ACTD binding. It is interesting to note that the ACTD binding affinities for members of the CTAG series are generally lower than the corresponding CATG counterparts, suggesting possible interesting sequence effects.

*ACTD Also Binds Strongly to d(TGT**CAATTG**) and Related Oligomers with 2:1 Drug to Duplex Binding Stoichiometry*. If our speculated model on ACTD binding to d(TG*T***CATG**) is valid, it is expected that ACTD will bind even more strongly to d(TG*T***CAATTG**) with similar binding densities, a consequence of the facilitated slipped duplex formation with 6 base pairs instead of 4. This oligomer is expected to form a duplex stem at the self-complementary hexanucleotide sequence CAATTG, and two ACTD molecules should be expected to bind at the duplex ends, utilizing the aforementioned binding principle. Indeed, a binding constant of 12×10^6 M^{-1} is found for d(TG*T***CAATTG**), severalfold higher than that of d(TG*T***CATG**). Studies were also made with d(TG*T***CATATG**), d(TG*T***CACGTG**), d(TG*T***CTATAG**), d(TG*T***CTTAAG**), and d(TG*T***CTCGAG**), all showing binding constants on the order of 10×10^6 M^{-1} (see Table 3) with 2:1 drug to duplex binding stoichiometries

Comparisons with Some GpC-Containing Oligomers. If our proposed *T*-base displacement binding mode for the G*T*C-containing oligomers is correct, one would expect the corresponding oligomers with GC in place of G*T*C to exhibit similar binding behaviors since there will be no need for a base displacement during the binding. Thus, ACTD binding

Table 4: Binding and Melting Parameters of Some GpC-Containing Oligomers[a]

oligomer	K (μM^{-1})	T_m^0 (°C)	T_m (°C)
d(TG**CATG**)	1.03 ± 0.06		41
d(TG**CTAG**)	0.45 ± 0.02		40
d(TG**CAATTG**)	6.6 ± 0.9		56
d(TG**CATATG**)	8.0 ± 0.7		57
d(TG**CACGTG**)	4.0 ± 0.6		51
d(TG**CTATAG**)	3.9 ± 0.2		53
d(TG**CTTAAG**)	2.5 ± 0.4		54
d(TG**CTCGAG**)	5.1 ± 0.3		49

[a] Equilibrium titrations were carried out at 25 °C, and the binding constant K is obtained via nonlinear least-squares fit to the experimental isotherm using the simple 1:1 binding model. T_m^0 and T_m are melting temperatures of 40 μM (in nucleotide) DNA/0.1 M NaCl in the absence and in the presence of 7 μM ACTD, respectively. The melting profiles were obtained via 275 nm absorbance monitoring.

studies were also made with oligomers having G*T*C replaced by GC, and the results of the nonlinear least-squares fits are summarized in Table 4. The binding isotherms (not shown) of these oligomers appear to be adequately fitted by the 1:1 drug to strand binding model (despite the presence of TGCA sites and the expectation of ACTD binding at these sites in some oligomers), suggesting a similar binding mode to that of G*T*C counterparts. Interestingly, the ACTD binding affinities for these GC-containing oligomers appear to be uniformly weaker than the corresponding G*T*C counterparts, suggesting possible roles played by the displaced *T*-bases in ACTD binding to G*T*C sites.

Melting and CD Spectral Characteristics. The extent of melting temperature increase of an oligomer upon ACTD binding can also serve as a qualitative measure of its binding affinity. Unfortunately, melting profiles for most of the oligomers studied are rather broad and diffuse, with no evidence of cooperative melting. Thus, their melting temperatures are difficult to extract. The drug−DNA complexes, however, exhibit cooperative melting profiles, and their melting temperatures can be easily obtained. The extracted melting temperatures for drug complexes have also been included in all the tables for comparison, and their values can be seen to qualitatively correlate with the strengths of ACTD binding. For example, the dramatic 28 °C melting temperature increases upon ACTD binding to both d(TG*T*-**CATG**AC) and d(TG*T***CATG**ACA) are consistent with two drug molecules binding to a duplex, since a single drug binding to a GpC site rarely exceeds a 20 °C increase. Representative melting profiles are compared in Figure 5 for d(TGT**CATG**TC) in the absence and in the presence of ACTD along with the drug-bound d(TGT**CATG**) and d(TGT**CATG**TCA). As is apparent, d(TGT**CATG**TC) exhibits a rather broad melting profile with little evidence of cooperative melting, In the presence of ACTD, however, a monophasic melting behavior is apparent even for d(TGT-**CATG**). The progressive melting temperature increases for the drug-bound complexes upon appending TC and TCA to the 3′-end can also be clearly seen by the progressive shifting of the melting profiles to higher temperatures.

In principle, the extent of melting temperature increase upon drug binding could also be used to estimate the binding constant. This can be accomplished by employing the equations of Crothers (*18*) and of McGhee (*19*) in which the melting temperatures in the absence (T_m^0) and in the

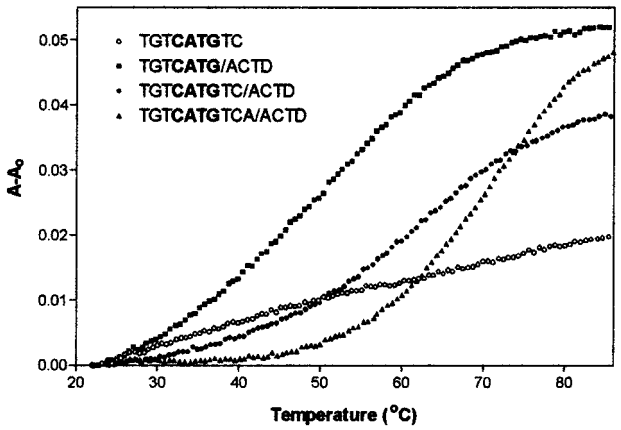

FIGURE 5: Comparison of thermal melting profiles of d(TGT**CAT-G**TC) in the absence and in the presence of ACTD along with drug complexes of d(TGT**CATG**) and d(TGT**CATG**TCA). DNA and drug concentrations are 40 μM (in nucleotide) and 7 μM, respectively. All solutions contain 0.1 M NaCl, and the absorbance monitoring was made at 275 nm, with a heating rate of 0.5 °C/min being maintained by the temperature controller accessory. Absorbance measured at the lowest temperature (A_o) was subtracted for easier comparison.

presence (T_m) of drug are related to the binding constant (K) and the free ligand activity (L) by the equation:

$$1/T_m^{\,0} - 1/T_m = R \ln (1 + KL)^n/\Delta H$$

where ΔH is the enthalpy change for the melting of a duplex and n is the number of binding sites per duplex. Unfortunately, a systematic comparison of such calculated results with our binding constants obtained via titrations cannot be made because of our inability to measure the melting temperatures of most of the oligomers studied. It is instructive to make such a comparison, however, with the only self-complementary oligomer studied in this report. $T_m^{\,0}$ and T_m for d(TGTCATGACA) were found to be 34 and 62 °C, respectively (see Table 1). Using a ΔH of 237 kJ/mol estimated from the nearest-neighbor thermodynamic data of Breslauer et al. (*20*) and an L of 4 μM and $n = 2$, a binding constant of 12×10^6 M^{-1} was estimated. This value compares favorable to that of 6.5×10^6 M^{-1} from our titration result (see Table 1), considering tabulated thermodynamic values to be those of 25 °C and 1 M NaCl in contrast to our experimental condition of 0.1 M NaCl.

ACTD binding also induces a substantial CD spectral alteration in the DNA spectral region. Thus, induced CD spectral characteristics can also provide some insights into the binding processes. A typical CD spectral alteration is illustrated with d(TGT**CATG**TCA) in Figure 6A. In the absence of ACTD, the oligomer exhibits a moderate bisignate CD spectrum with positive and negative maxima near 280 and 255 nm, respectively. Upon binding to ACTD, however, a moderately positive CD and a strongly negative CD are induced near 293 and 253 nm, respectively. The effect can be seen more clearly by the difference spectrum with the DNA contribution subtracted out. A shoulder near 270 nm is clearly evident in such a spectrum. The significance of this shoulder is made more apparent by a difference spectral comparison of d(TGT**CATG**) and d(TG**CATG**) in Figure 6B. The prominent presence of the 270 nm shoulder of the former in contrast to its near-absence of it in the latter

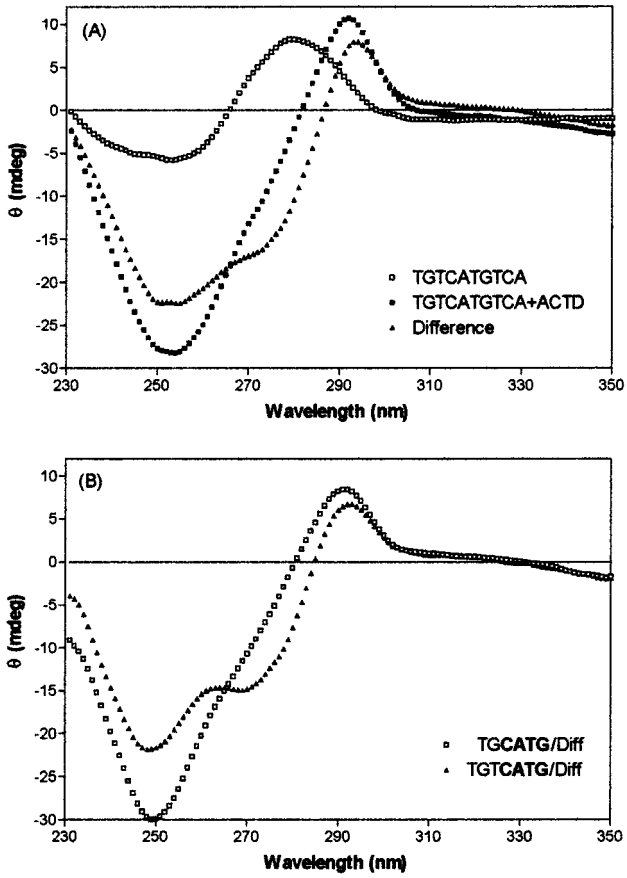

FIGURE 6: (A) CD spectral comparisons of 40 μM (in nucleotide) d(TGT**CATG**TCA) in the absence and in the presence of 7 μM ACTD. The difference spectrum is obtained by subtracting the DNA contribution from that of DNA+ACTD. (B) Comparison of difference CD spectra of d(TGT**CATG**) vs d(TGT**CATG**) to highlight their differential effect upon ACTD binding. All CD measurements were made at room temperature using cylindrical cells of 2 cm path length.

suggests that it may be characteristic for the binding at the GTC/G or GTC/GTC site, highlighting the effect of the looped-out T-base. CD titrations with progressive additions of ACTD were not attempted, as ACTD is optically active and exhibits weak but significant CD in this spectral region.

DISCUSSION

Our results indicate that ACTD binds well to d(TG*T*-**CATG**) and strongly to d(TG*T***CATG**TC) and d(TG*T***CAT-G**TCA) with a 2:1 drug to duplex binding stoichiometry. These oligomers contain no GpC sequences, yet their binding affinities are comparable to or higher than the GpC-containing oligomers. The ACTD binding to d(TG*T***CATG**) is rationalized in terms of a binding mode in which the oligomer forms a slipped dimeric duplex at the self-complementary CATG sequence and the ACTD molecules stack on each end of the duplex stem while the other face of the drug chromophore is stacked by the 3′-side of the dangling G-base with a loop-out *T*-base. The greatly enhanced ACTD affinities with TC and TCA additions at the 3′-end can be viewed as the consequence of facilitating such a stereo-geometry by stabilizing the G*T*C/G*T*C sites via extra base pair(s) formation. It is further supported by the finding that, although the binding is also enhanced by the AC and ACA additions, the effects are only nominal and their ACTD

affinities are considerably weaker than the corresponding TC and TCA counterparts. This is due to the T·A base pair formation at the G*T*C/G*A*C site, which somewhat hinders base displacements for ACTD binding at these sites. It is, nonetheless, remarkable that the affinity for ACTD forces the disruption of the *T*·*A* base pair.

Additional support for the base-displacement model comes from the observation that the replacement of G*T*C by G*TT*C led to a considerably weaker binding due to the added difficulty in displacing an additional *T*-base. And similar binding behavior should have been expected for d(TG**CATG**) since there will be no need to displace the T-base for such a binding. Indeed, a binding density of 2:1 drug to duplex is found rather than 1:1 for this oligomer, indicating ACTD being bound at the slipped duplex formed at the CATG rather than intercalation at the duplex formed at the TGCA sequence. Interestingly, instead of an expected stronger binding than its GTC counterpart, d(TG**CATG**) in fact binds severalfold weaker than d(TG*T***CATG**), and the melting temperature of the drug complex was found to be about 10 °C lower. This likely suggests some sort of interaction of ACTD with the looped-out base in further stabilizing the GTC complex.

Due to the small numbers of base pairs in the slipped duplex formation on the sequences studied, most of the oligomers studied inevitably exist in multiple conformational states in solutions and exhibit little cooperative melting. Despite the fact their drug binding resulted in greatly enhanced duplex stability, their melting temperatures cannot be used to estimate binding constants quantitatively and to compare with the values obtained via spectral titrations. Attempts were made to investigate the relative contributions of various conformers in solutions via capillary electrophoresis, but without success. Single broad peaks were observed for most oligomers with migration times shorter than the duplex standard, likely the consequence of rapid exchange among various conformers.

Our proposed binding model makes use of the notion that ACTD prefers to have the 3′-sides of both G-bases stacked on the opposite faces of its planar phenoxazone chromophore (*2*, *21*). Such a binding principle is akin to the classic notion of ACTD preference at the GC *duplex* site, which can be viewed as stabilizing the required stereo-geometry of two G-bases via G·C base pair formation. Based on this binding principle and the results of CATG and CTAG analogues, it is only natural to anticipate that ACTD would also bind tightly to oligomers of sequence motifs d(TGTCxyy′x′G), where x′ and y′ are complementary to x and y, respectively, and y $\neq$ G. These predictions have been borne out by experiments. Indeed, oligomers d(TG*T***CAATTG**), d(TG*T***CATATG**), d(TG*T***CACGTG**), d(TG*T***CTATAG**), d(TG*T***CTTAAG**), and d(TG*T***CTCGAG**) all exhibit binding constants of roughly 1×10^7 M^{-1} with 2:1 drug to duplex binding stoichiometry. The somewhat greater ACTD binding affinities of these oligomers as compared to those of d(TG*T***CATG**) and d(TG*T***CTAG**) are likely the consequence of the more stable slipped duplex formation, 6- vs 4-base-paired stem.

Crystallographic analysis of a novel complex of ACTD bound to DNA decamer d(CGATCGATCG) has just appeared in print (*22*). It is gratifying to note that the structure of the complex is akin to our model with ACTD stacking at both ends of the slipped duplex formed at the CGATCG sequence, with stacking of the dangling G-bases on the other faces of the phenoxazone planes via swing-out AT bases. The novel structure of the complex resembles strikingly that of the elongation locus during transcription, and its implication on the transcription inhibitory process has been speculated (*22*).

REFERENCES

1. Muller, W., and Crothers, D. M. (1968) *J. Mol. Biol. 35*, 251−290.
2. Sobell, H. M., and Jain, S. C. (1972) *J. Mol. Biol. 68*, 21−34.
3. Kamitori, S., and Takusagawa, F. (1992) *J. Mol. Biol. 225*, 445−456.
4. Chen, F.-M. (1988) *Biochemstry 27*, 6393−6397.
5. Chen, F.-M. (1992) *Biochemstry 31*, 6223−6228.
6. Liu, C., and Chen, F.-M. (1996) *Biochemistry 35*, 16346−16353.
7. Snyder, J. G., Hartman, N. G., D'Estantoit, B. L., Kennard, O., Remeta, D. P., and Breslauer, K. J. (1989) *Proc. Natl. Acad. Sci. U.S.A. 86*, 3968−3972.
8. Rill, R. L., Marsch, G. A., and Graves, D. E. (1989) *J. Biomol. Struct. Dyn. 7*, 591−604.
9. Bailey, S. A., Graves, D. E., and Rill, R. (1994) *Biochemistry 33*, 11493−11500.
10. Wadkins, R. M., and Jovin, T. M. (1991) *Biochemistry 30*, 9469−9478.
11. Hsieh, Y. L., Li, Y. T., and Henion, J. D. (1994) *Biol. Mass Spectrom. 116*, 272−276.
12. Wadkins, R. M., Jares-Erijman, E. A., Klement, R., Rudiger, A., and Jovin, T. M. (1996) *J. Mol. Biol. 262*, 53−68.
13. Rill, R. L., and Hecker, K. H. (1996) *Biochemistry 35*, 3525−3533.
14. Wadkins, R. M., Vladu, B., and Tung, C.-S. (1998) *Biochemistry 37*, 11915−11923.
15. Sha, F., and Chen, F.-M. (2000) *Biophys. J. 79*, 2095−2104.
16. Chen, F.-M., and Sha, F. (2001) *Biochemistry 40*, 5218−5225.
17. Fassman, G. D., Ed. (1975) *CRC Handbook of Biochemistry and Molecular Biology*, 3rd ed., Vol. I, p 589, CRC Press, Cleveland, OH.
18. Crothers, D. M. (1971) *Biopolymers 10*, 2147−2160.
19. McGhee, J. D. (1976) *Biopolymers 15*, 1345−1375.
20. Breslauer, K. J., Frank, R., Blocker, H., and Marky, L. A. (1986) *Proc. Natl. Acad. Sci. U.S.A. 83*, 3746−3750.
21. Krugh, T. R., and Neely, J. W. (1973) *Biochemistry 12*, 4418−4425.
22. Robinson, H., Gao, Y.-G., Yang, X.-L., Sanishvili, R., Joachimiak, A., and Wang, A. H.-J. (2001) *Biochemistry 40*, 5587−5592.

BI011787O